

# Preservation of Ganglion Cell Layer Neurons in Age-Related Macular Degeneration

Nancy E. Medeiros<sup>1</sup> and Christine A. Curcio<sup>2</sup>

**PURPOSE.** To determine the number of neurons remaining in the ganglion cell layer (GCL) of eyes with nonexudative and exudative age-related macular degeneration (NEAMD and EXAMD, respectively) in relation to photoreceptor loss in the same retinas.

**METHODS.** The study design was a clinicopathologic correlation. Macular photoreceptors and GCL neurons were counted in unstained retinal wholemounts from eyes of patients with NEAMD ( $n = 6$ ) and EXAMD ( $n = 5$ ) and from control patients without grossly visible drusen or pigmentary change ( $n = 15$ ; age range, 60–95 years). The authors determined the percentage of counting sites with significant cell loss relative to control eyes and for photoreceptors, the percentage of sites where rod or cone loss predominated. The total numbers of cones, rods, and GCL neurons were determined within the 6-mm-diameter macula. Fellow eyes were prepared for light and electron microscopic evaluation of retinal pigment epithelium and Bruch's membrane disease.

**RESULTS.** EXAMD eyes had severe photoreceptor loss. The total number of macular photoreceptors in NEAMD eyes was similar to the number in control eyes, despite moderate loss in the parafovea. In 9 of 11 AMD eyes, rod loss was greater than cone loss at the same locations. EXAMD eyes had 47% fewer GCL neurons than control eyes. GCL neurons in NEAMD eyes did not differ significantly from control eyes.

**CONCLUSIONS.** Interventions targeted at the outer retina early in the progression of neovascular disease should benefit from the full age-appropriate complement of GCL neurons. (*Invest Ophthalmol Vis Sci.* 2001;42:795–803)

Visual rehabilitation of patients with severe photoreceptor loss using tissue<sup>1</sup> or electronic prostheses<sup>2</sup> requires an adequately functioning ganglion cell layer (GCL) for signal transmission to the brain. Transneuronal degeneration of the GCL subsequent to photoreceptor death could substantially reduce the potential benefits of these future therapies. Inner retinal survival after disease-related photoreceptor loss is best documented for retinitis pigmentosa (RP),<sup>3–5</sup> a clinical phenotype common to many inherited disorders.<sup>6,7</sup> In the maculas of patients with RP, the number of surviving GCL neurons is 30% to 75% that in control eyes, with evidence that the most severe cases have the fewest surviving neurons. These same eyes have

fewer GCL neurons surviving in the peripheral retina than in the macula, with 30% of GCL neurons remaining in moderate cases and 20% remaining in severe cases.<sup>5</sup>

Age-related macular degeneration (AMD) is the leading cause of untreatable new vision loss in the older population.<sup>8–10</sup> Nonexudative AMD (NEAMD) is characterized by gradual vision loss associated with retinal pigmentary change, drusen, and the development of geographic atrophy of the retinal pigment epithelium (RPE).<sup>11</sup> The exudative form of AMD (EXAMD) is responsible for rapid and severe vision loss due to the development of choroidal neovascularization (CNV).<sup>11</sup> Loss of photoreceptors is associated with both forms of AMD,<sup>12</sup> but there is little information about GCL status in the retinas of patients with AMD. One study detected almost complete loss of macular GCL neurons in two eyes of one patient with AMD,<sup>13</sup> but because of the small sample and because there were no control eyes it is not known how GCL status varies with stage of AMD or among individual patients. Our previous histopathologic study of macular photoreceptors in AMD showed moderate loss in the parafovea in NEAMD and severe but not complete loss in late AMD.<sup>12</sup> If GCL neurons are lost because of transneuronal degeneration subsequent to disease-related photoreceptor death, then we expect that loss of GCL neurons is greater in EXAMD than in NEAMD, because of the greater photoreceptor loss in late AMD. We tested this hypothesis by counting photoreceptors and GCL neurons in wholemounted retinas from 6 eyes with NEAMD, 5 eyes with EXAMD, and 15 age-matched control eyes.

## METHODS

Our results are based on 21 eyes obtained after death from 11 patients with AMD (Table 1). Twelve eyes from six patients, previously characterized with respect to histopathology and photoreceptor loss,<sup>12</sup> and nine eyes from five new patients produced similar results and are presented together. Informed consent to eye donation and release of medical records were obtained from next of kin. Procedures involving human tissues and medical records were approved by institutional review at the University of Alabama at Birmingham and adhered to the tenets of the Declaration of Helsinki.

Eyes were preserved quickly after death ( $n = 11$ , <5 hours;  $n = 10$ , <3 hours). After removal of the anterior segment, eyes of each donor or patient were preserved by immersion in 0.1 M phosphate buffered (PB) fixative. One eye from each donor was used for histopathologic diagnosis of AMD, and the fellow eye was used for cell-counting studies. Comparison of data from fellow eyes in this manner was justified, because the two eyes of each donor were similar in gross fundus appearance and available clinical history and because age-related macular change is typically bilateral.<sup>12,14–16</sup> Preserved globes were viewed internally and photographed with a stereomicroscope using front and back lighting to assess the presence of drusen and pigmentary disturbances.<sup>12,17</sup>

Ten eyes from 11 donors with AMD were sectioned for light microscopic histopathologic evaluation. These eyes were preserved in either 4% paraformaldehyde ( $n = 7$ ), 4% paraformaldehyde and 0.5% glutaraldehyde ( $n = 1$ ), or 1% paraformaldehyde and 2.5% glutaraldehyde ( $n = 2$ ). From seven eyes (cases 3–6, 9–11) a piece of retina, RPE, choroid, and sclera containing the macula and optic nerve head was

---

From the <sup>1</sup>Retinal Specialists of North Alabama (formerly Retina and Vitreous Associates of Alabama, Huntsville); and the <sup>2</sup>Department of Ophthalmology, University of Alabama at Birmingham.

Supported in part by National Institutes of Health Grants EY06109 (CAC) and P30 EY03039 (Vision Science Research Center, University of Alabama at Birmingham), Helen Keller Eye Research Foundation (NEM), and unrestricted grants from Research to Prevent Blindness, and the Alabama Eye Institute to the Department of Ophthalmology.

Submitted for publication August 15, 2000; revised November 22, 2000; accepted November 30, 2000.

Commercial relationships policy: N.

Corresponding author: Christine A. Curcio, Department of Ophthalmology, University of Alabama at Birmingham, Eye Foundation Hospital, Rm H20, 700 South 18th Street, Birmingham AL 35294-0009. curcio@uab.edu

TABLE 1. Eyes Studied

Case	Age (y)	Sex	Last Examination*	Last Acuity	FA	Ocular History	Histopathology, Fellow Eye†
Eyes with NEAMD							
1	69	M	1	20/25	N	Drusen and pigment change, mild cataract	D, C
2	74	M	19	20/25	Y	Dry AMD, mild EMP, mild cataract	D
3	79	F	NA	Good vision	N	No visual symptoms, according to family, mild cataract	D, BD, C, A
4	81	M	8	20/40	Y	AMD, potential acuity meter 20/20, cataract	BD, C, A
5	87	M	42	20/30	N	AMD, pseudophakic cystoid macular edema	D, BD
6	93	F	63	20/60	N	Tigroid macula without drusen, dense nuclear cataract	D, BD
Eyes with EXAMD							
7	74	M	3	CF	Y	EXAMD, recurrent CNV after laser, moderate cataract	BD, GA, DS
8	76	M	5	CF 6 ft.	N	AMD, significant cataract	NA
9	85	M	1	<20/400 ecc	Y	EXAMD, used low vision aids	D, BD, GA, DS
10	90	M	>60	"Barely see"	N	Poor vision for 25 years according to family; "inoperable retina problem"	BD, GA, DS
11	93	F	NA	LP	N	Cataract	BD, GA, DS

FA, fluorescein angiogram; EMP, epimacular proliferation; CF, count fingers; LP, light perception; NA, not available; D, drusen  $>63 \mu\text{m}$ ; BD, continuous basal deposits; C, RPE clumping; A, nongeographic RPE atrophy; GA, geographic RPE atrophy; DS, disciform scar.

\* Months before death or surgery.

† Histopathology notes.

embedded in medium (JB-4; Polysciences, Warrington, PA). Serial  $3\text{-}\mu\text{m}$  sections were stained with Richardson's stain. The foveas of three eyes (cases 1, 2, and 7) were embedded in epoxy resin. One-micrometer sections were stained with toluidine blue, and ultrathin sections were examined by electron microscopy.

Foveal sections from all eyes were evaluated for the presence of drusen, basal deposits, RPE change, choroidal neovascularization, and disciform degeneration, using a semiquantitative grading scheme.<sup>17</sup> AMD cases were defined using histopathologic criteria. NEAMD had either one druse more than  $63 \mu\text{m}$  in diameter or severe RPE change (clumping, anterior migration, or atrophy). Eyes with changes in the

RPE also had to have at least one druse or a continuous layer of basal deposits. Eyes with EXAMD had choroidal neovascularization and/or fibrovascular scars with basal deposits or drusen. Clinical records were reviewed to eliminate eyes with other macular chorioretinal diseases and eyes with glaucoma.

Eleven retinas from 11 donors with AMD were prepared for quantification of photoreceptors and GCL neurons (study eyes). Methods used for our previous study of photoreceptor density in six AMD eyes<sup>12</sup> were used for the five AMD eyes added for the present study. Photoreceptors and GCL neurons were counted in unstained wholemounts. This method is preferable to histologic sections for quantifying retinal

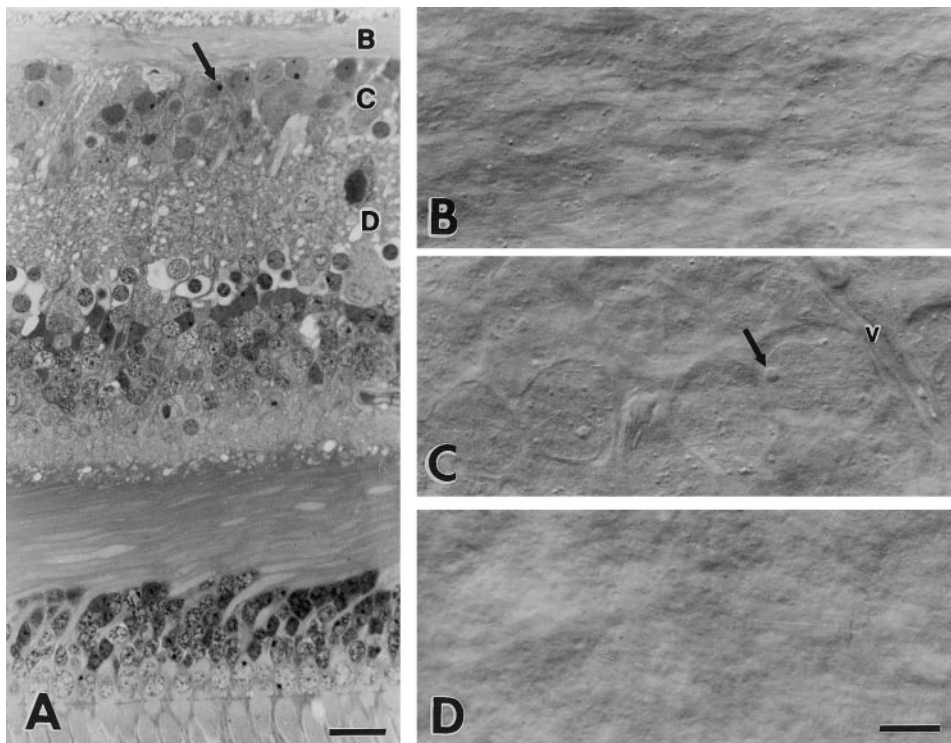
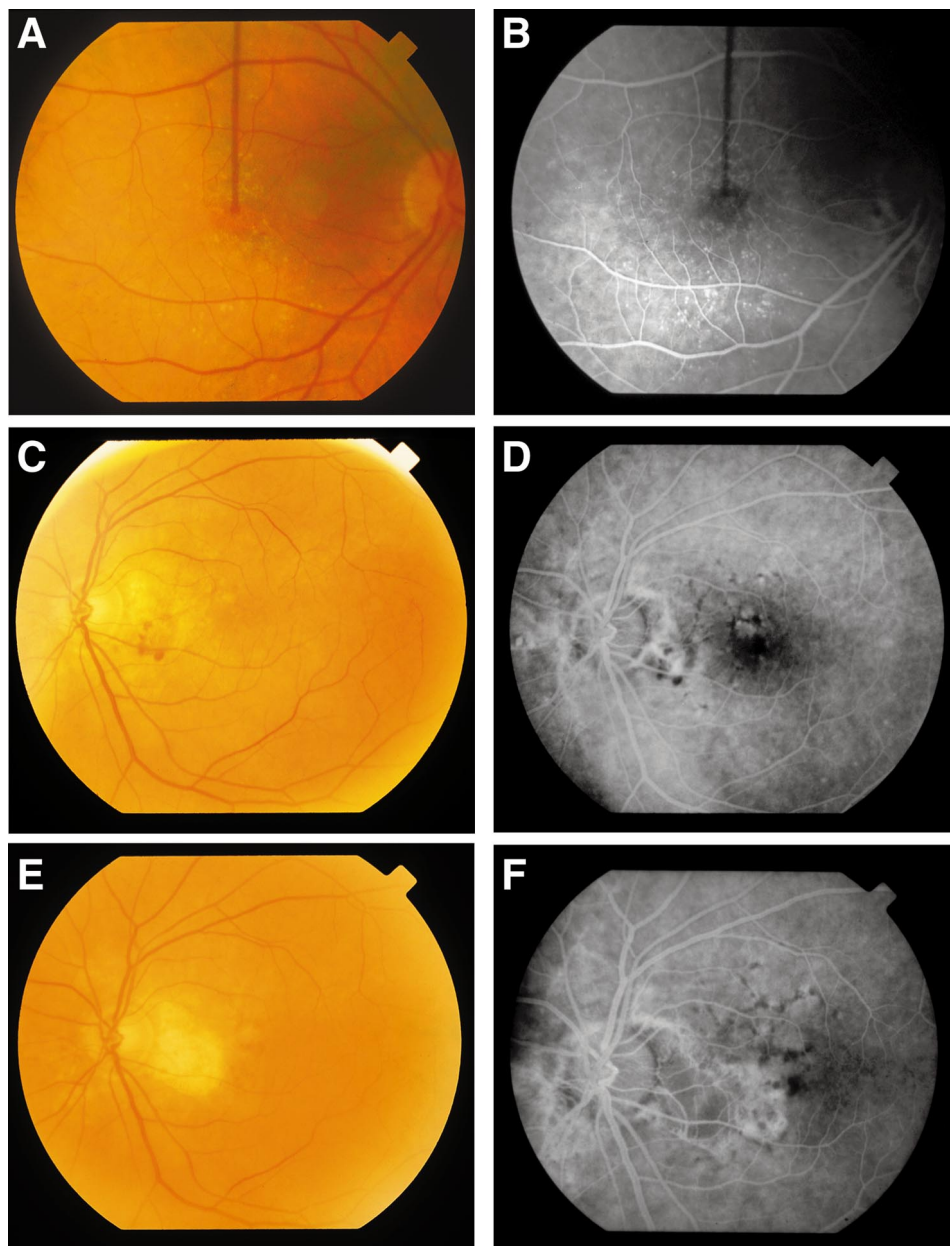


FIGURE 1. GCL in a normal human macula, in a vertical histologic section (A,  $1\text{-}\mu\text{m}$ -thick section, toluidine blue), and horizontal optical sections (B, C, and D, unstained wholemount, Nomarski optics). In (A), B, C, and D refer to the layers shown as focal planes in panels (B), (C), and (D). (B) Inner plexiform layer; (C), GCL; (D), nerve fiber layer. Arrows: Nucleoli of GC; v, small vessel. Scale bars, (A)  $20 \mu\text{m}$ ; (B, C, and D)  $10 \mu\text{m}$ .



**FIGURE 2.** Fundus photographs and fluorescein angiograms (FA) of AMD eyes. NEAMD case 2: (A) Drusen typical of NEAMD; (B) corresponding FA showing staining of drusen but no dye leakage. EXAMD case 7, September 1991: (C) Confluent soft drusen and peripapillary subretinal hemorrhage; (D) corresponding FA showing extrafoveal peripapillary CNV. EXAMD case 7, August 1992: (E) Peripapillary laser scar with faint subretinal hemorrhage on the temporal edge; (F) corresponding FA revealing recurrent subfoveal CNV with hyperfluorescence extending from the old laser scar.

cells, because it preserves cellular morphology and retinal topography, minimizes tissue shrinkage, and permits resolution of individual GCL neurons even in the densely packed foveal GCL.<sup>12,18–21</sup> These eyes were preserved in either 4% paraformaldehyde ( $n = 5$ ) or 4% paraformaldehyde and 0.5% glutaraldehyde ( $n = 6$ ), both of which produced excellent optical clarity for the quantitative studies performed. In eight AMD eyes, the macular retina and optic nerve head were separated from the RPE-choroid and disciform scar. In three AMD eyes (cases 1, 2, and 6), the RPE-choroid was left attached and bleached overnight with buffered 10% hydrogen peroxide. All retinas were cleared with 100% dimethyl sulfoxide and mounted with polyvinyl alcohol and glycerol. Retinas were initially mounted with the photoreceptor layer on top for photoreceptor counts. They were remounted with the GCL on top for GCL counts.

For cell counts, unstained wholemounts were viewed with a combination of Nomarski differential interference contrast (NDIC) optics and video. In the photoreceptor layer, we counted cells at the level of inner segments, as previously described.<sup>12,18,20,21</sup> Cones were distinguished from rods by the threefold larger diameter of their inner segments, a difference that persisted in diseased eyes.<sup>12</sup> The GCL could

be distinguished from the fibrous nerve fiber layer and the granular inner plexiform layer in optical sections at different focal planes,<sup>19</sup> as shown in Figure 1. Nonneural cells in the GCL (i.e., endothelial cells, pericytes, and presumed astrocytes<sup>22–25</sup>) could be distinguished from neurons by their laminar location, small size, and nuclear morphology. In the GCL, nucleoli were counted.<sup>19</sup> GCL neurons included a majority population of cells with large somata relative to their nuclei (ganglion cells) and a minority population of cells with small somata relative to their nuclei (displaced amacrine cells).<sup>19,20</sup> Displaced amacrine cells represent 3% to 10% of the total GCL population in the primate macula.<sup>26</sup> In this study, counts of GCL neurons included ganglion cells and displaced amacrine cells.

We counted photoreceptors and GCL neurons with a computer-video-microscope system that included a  $60 \times 1.4$  numeric aperture oil-immersion objective, NDIC optics, a digitizing tablet, and a computer-controlled stepper motor stage. We systematically sampled the macula to capture the steep gradients of macular cell density and obtain an accurate measure of total cell number.<sup>18,19</sup> In NEAMD and control eyes, we counted photoreceptors at 100 to 120 locations that were closely spaced in the fovea and less closely spaced away from the



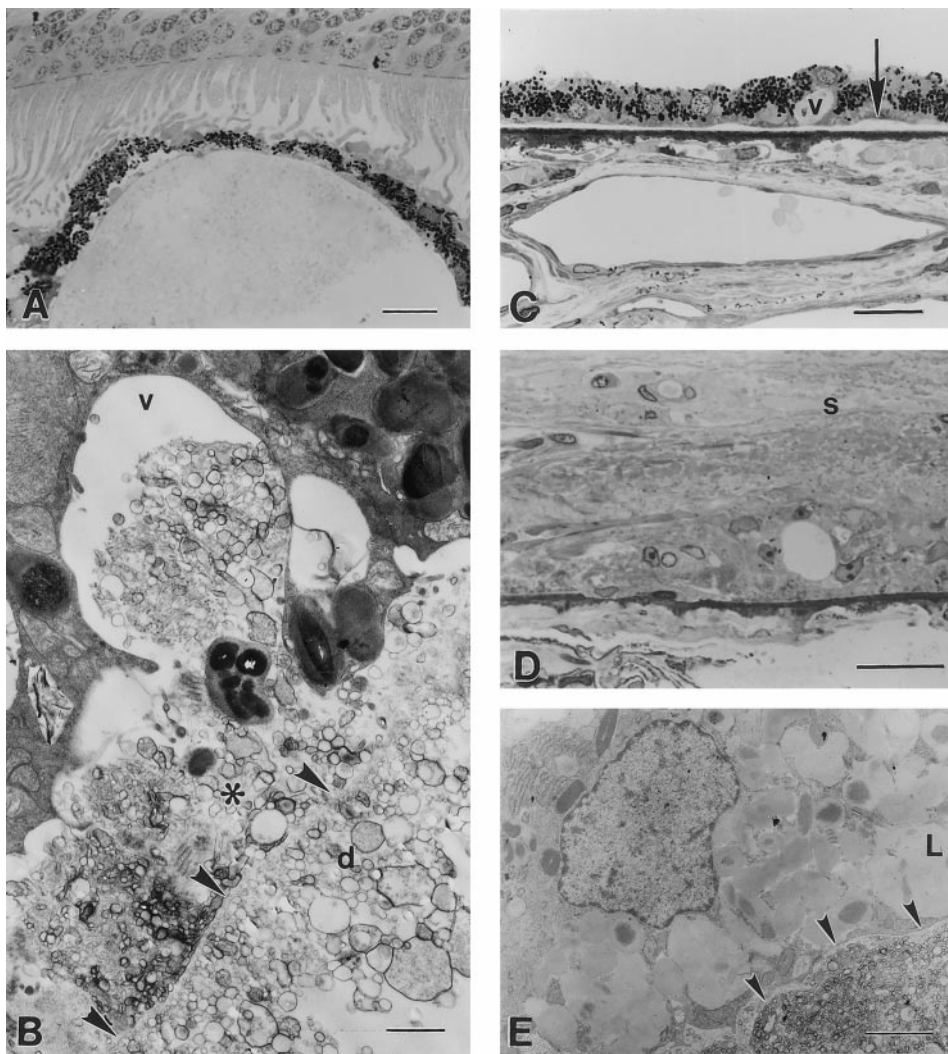


**FIGURE 3.** Histopathology and ultrastructure of eyes with NEAMD and EXAMD. (A) Large druse in case 2. (B) Membranous debris in druse (d), basal laminar deposit (\*), and vacuole (v) in case 2. (C) Intracellular vacuole and layer containing membranous debris (basal linear deposit, arrow) in case 1. (D) Fibrovascular scar (S) and cells in case 7. (E) RPE cell overlying membranous debris in case 7. (A), (C), and (D) are light micrographs of 1- $\mu$ m sections, toluidine blue stain; (B) and (E) are electron micrographs; arrowheads: RPE basal lamina. RPE is at the top, and choroid is at the bottom of all panels. Bars, (A, B, and D) 20  $\mu$ m; (C, E) 1  $\mu$ m.

fovea. At each location, we counted photoreceptors in a single 39- $\mu$ m<sup>2</sup> counting window at a viewing magnification of  $\times 3000$  on the video monitor. In EXAMD eyes, we counted photoreceptors by using a different sampling strategy, because there were large areas of nearly complete photoreceptor loss vitread to fibrovascular scars. We counted photoreceptors along meridians extending peripherally from the margin of the degenerated area into an intact mosaic of recognizable photoreceptor inner segments. We expressed the extent of severe photoreceptor degeneration as the distance from the foveal center (recognized by inner retinal landmarks) to the intact photoreceptor layer. In all eyes, we counted GCL neurons at locations in a sampling pattern similar to that used for photoreceptors in NEAMD eyes. At each location, we counted GCL neurons in adjacent 39- $\mu$ m<sup>2</sup> windows until a total of 15 cells was obtained.

We analyzed counts of photoreceptors and GCL neurons in two ways, as previously described.<sup>12,20,21</sup> First, we compared the density of cones, rods, and GCL neurons at retinal locations in diseased eyes to matched locations in control eyes that had no grossly visible macular drusen and pigmentary change (for photoreceptors,<sup>21</sup>  $n = 12$ , age range, 61–90 years; for GCL neurons,<sup>20,27</sup>  $n = 15$ ; age range, 60–95 years). At each location, we computed the mean of  $\log(\text{AMD cell density}/\text{control cell density})$  for pair-wise comparisons of each AMD eye and five to eight appropriately age-matched control eyes. We generated a 95% confidence interval for the variability in cell density among control eyes by comparing the control eyes with each other in the same way. We considered differences between an AMD eye and control eyes that were below the lower confidence limit for control

eyes to show significant loss. For AMD eyes, we report the percentage of counting sites with significant loss, and for photoreceptors, the percentage of sites with loss in which rod or cone loss predominated. Second, we computed the total number of cones, rods, and GCL neurons within the 6 mm-diameter macula by integrating cell density over this region in AMD and control eyes. We also computed the total number of cones within the 0.8-mm-diameter, cone-dominated region of the fovea.<sup>18,21</sup> We assessed differences in the total number of macular photoreceptors and GCL neurons in the NEAMD, EXAMD, and control groups by a single factor analysis of variance, with  $P < 0.05$  considered significant.

## RESULTS

Clinical data from the 11 study eyes are summarized in Table 1. Similar to previously presented cases,<sup>12</sup> the additional eyes used for this study (cases 1, 2, 6, 7, and 8) were obtained from white patients with a history of bilateral AMD. Two patients died of cancer but did not have symptoms of cancer-associated retinopathy. As previously reported,<sup>12</sup> the NEAMD group demonstrated more preservation of useful vision than the EXAMD group.

Fundus photographs of eyes in case 2 (NEAMD) obtained before death are shown in Figures 2A and 2B. This 74-year-old man was referred to a retina specialist in March, 1993, because of new visual distortion. On examination, visual acuity mea-

TABLE 2. Cell Loss

	NEAMD Cases						EXAMD Cases				
	1	2	3	4	5	6	7	8	9	10	11
<b>Photoreceptors</b>											
Severe degeneration, V diameter (mm)*	—	—	—	—	—	—	9.4	1.8	4.0	9.0	4.5
Severe degeneration, H diameter (mm)*	—	—	—	—	—	—	9.2	2.0	4.2	12.0	5.6
Sites with significant loss (%)†	33	58	52	59	52	50	81	68	84	88	46
Sites with C loss > R loss (%)‡	35	100	21	27	72	11	27	10	41	41	29
Sites with R loss > C loss (%)‡	65	0	79	73	28	89	73	90	59	59	71
Total cones, fovea§	27.4	25.1	33.7	—	27.4	31.7	—	—	—	—	—
Total cones, macula	298.1	263.8	279.6	306.2	247.1	354.7	—	—	—	—	—
Total rods, macula	2353.3	2998.1	1572.8	1607.6	1739.6	1554.8	—	—	—	—	—
<b>GCL Neurons</b>											
Sites with significant loss (%)†	7	4	64	8	1	3	96	8	68	42	74
Total GCL neurons	386.1	409.0	229.0	330.9	410.5	353.8	141.5	325.4	151.6	233.6	160.0

—, Not applicable. V, vertical; H, horizontal; C, cone; R, rod.

\* Diameter of macular region without a confluent photoreceptor layer.

† Total sites with counts (27–170 for photoreceptors, 72 for GCL neurons).

‡ Sites with loss.

§ Total within 0.4 mm of foveal center,  $\times 1000$ ; total not available for case 4 because of processing-related damage in central 100  $\mu\text{m}$  of fovea.

|| Total within 3 mm of foveal center,  $\times 1000$ .

sured 20/25, and a fluorescein angiogram revealed NEAMD without leakage. On follow-up examination 6 months later, symptoms of worsening metamorphopsia prompted a second fundus photograph (Fig. 2A) and fluorescein angiogram (Fig. 2B), reconfirming NEAMD without CNV. On his last office visit in November 1994, the patient's vision remained 20/25 without clinical signs of CNV. No mention of new vision disturbances was noted before his death in June 1996.

Photographs of eyes in case 7 (EXAMD) are shown in Figures 2C through 2F. This 74-year-old man reported metamorphopsia in his left eye in September 1991. The color fundus photograph (Fig. 2C) at that time revealed confluent soft drusen and peripapillary subretinal hemorrhage. The corresponding fluorescein angiogram (Fig. 2D) revealed classic, extrafoveal CNV, which was treated with focal laser photocoagulation on the same day. Visual acuity in this eye remained at 20/30 until August 1992, then decreased to 20/50. A second color fundus photograph documented the creamy appearance and faint subretinal hemorrhage from recurrent CNV, extending from the temporal edge of the peripapillary laser scar (Fig. 2E). Confirmation of recurrent subfoveal CNV was obtained by fluorescein angiography (Fig. 2F). Laser treatment was not recommended. The patient's right (nonstudy) eye had a similar clinical history of EXAMD with recurrence after laser treatment. Visual acuity remained at count-fingers level in both eyes until the last clinical examination in May 1996, before the patient's death in September 1996.

The results of histopathologic evaluation of 10 AMD eyes are summarized in Table 1 and illustrated in Figure 3. NEAMD eyes had severe RPE changes, a continuous band of sub-RPE deposits, and drusen more than 63  $\mu\text{m}$  in diameter (Fig. 3A) that contained membranous debris (Fig. 3B). In addition to its location in drusen, membranous debris was also found in a thin layer within inner Bruch's membrane (basal linear deposit, Fig. 3C) and within intracellular vacuoles (Figs. 3B, 3C). EXAMD eyes had basal linear deposit, geographic atrophy of the RPE, and a fibrovascular scar containing numerous cells (Figs. 3D, 3E).

The topography of photoreceptor loss in the maculas of AMD eyes compared with control eyes is summarized in Table 2 and illustrated in Figures 4 and 5. Moderate photoreceptor loss was detectable at 33% to 82% of the extrafoveal counting sites in NEAMD eyes (Table 2), largely confined to an annulus

between 0.5 and 3 mm from the foveal center (Figs. 4A, 4B). As assessed by the percentage of sites with selective loss, rod loss predominated in four eyes (cases 1, 3, 4, 6), and cone loss

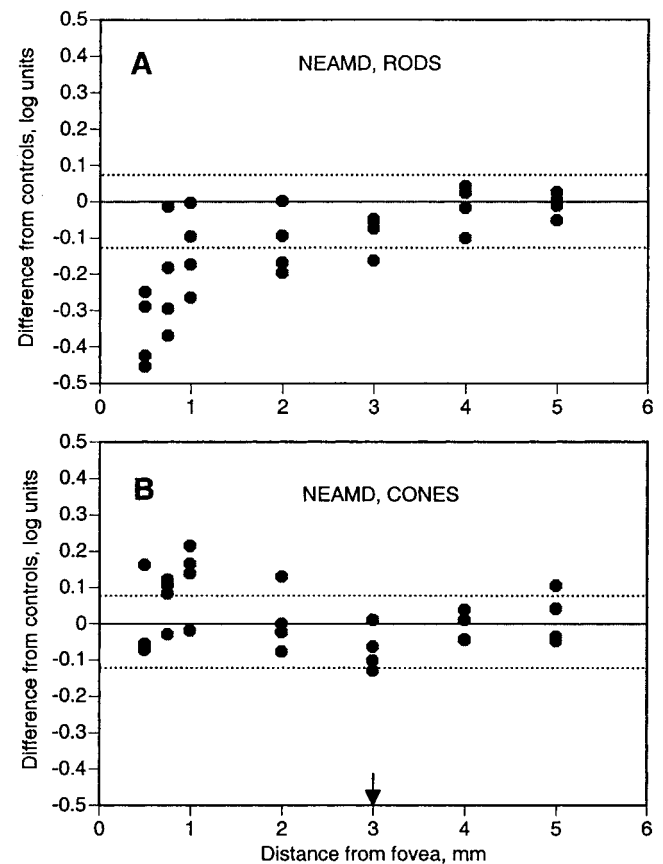


FIGURE 4. Loss of rods and cones as a function of distance from the foveal center in NEAMD case 6. Locations less than 0.5 mm from the foveal center, where rod densities are low and individual variability is high, are omitted. Dashed lines: The 95% confidence intervals obtained by comparing interspecimen densities of control eyes. Arrow, 3 mm: limits of macula.

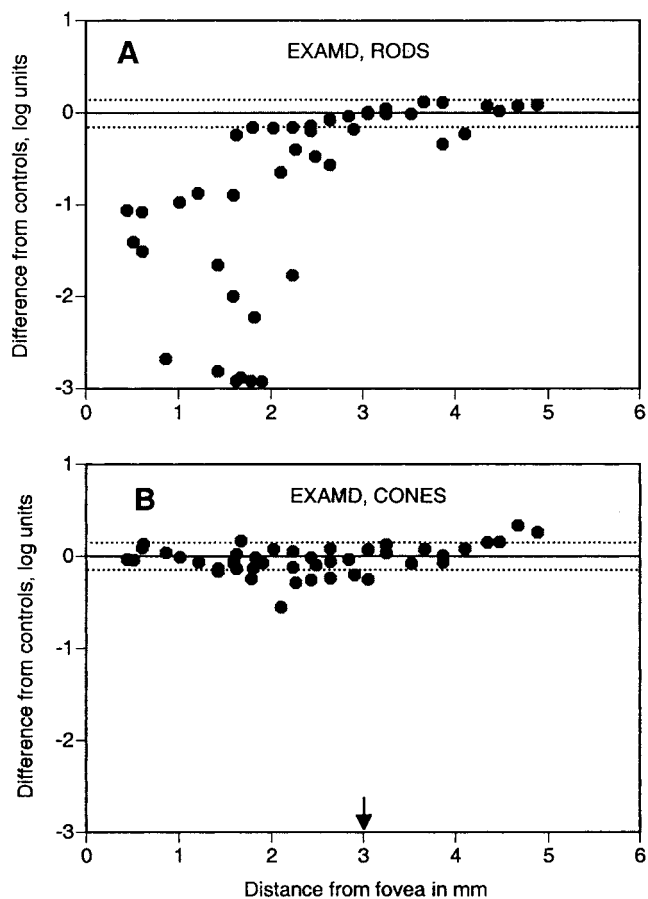


FIGURE 5. Loss of rods and cones as a function of distance from the foveal center in EXAMD case 8. See Figure 4 for details.

predominated in two (cases 2 and 5, Table 2). This regional loss, however, was insufficient to reduce the total number of macular photoreceptors in NEAMD eyes significantly below that of controls (Table 3). The number of foveal cones in NEAMD eyes did not differ significantly from control eyes (Table 2). In contrast to the NEAMD eyes, EXAMD eyes had a region 2.0 to 12.0 mm in diameter (Table 2) immediately vitreal to the fibrovascular scar in which photoreceptors had no outer segments and formed islands or rosette-like structures rather than a continuous layer. In the photoreceptor mosaic at the peripheral margin of fibrovascular scars, rod density declined precipitously, reaching very low levels near the margin in all EXAMD eyes (Table 2, Figs. 5A, 5B). Cone density had no relation to this boundary. Thus, EXAMD eyes in our sample had more severe loss of photoreceptors than did NEAMD eyes, but this loss was not complete. In 9 of 11 NEAMD and EXAMD eyes, rod loss was more severe than cone loss at corresponding locations (Table 2).

Contour maps of the mean density of GCL neurons in control, NEAMD, and EXAMD groups are shown in Figure 6. In

all three groups the density of GCL neurons was highest in a horizontally oriented elliptical ring 0.5 to 2 mm from the foveal center. In control and NEAMD eyes (Fig. 6A,B), cell densities peaked at 20,000 to 25,000 cells/mm<sup>2</sup> in this ring and decreased to less than 5000 cells/mm<sup>2</sup> at locations peripheral to the 6-mm diameter macula. Maximum cell densities in the EXAMD group (15,000–20,000 cells/mm<sup>2</sup>) were lower than either control or NEAMD groups, and isodensity contours were generally constricted (Fig. 6C). The number of counting sites with GCL neuron loss relative to controls is summarized in Table 2, and cell loss is plotted as a function of distance from the fovea in Figure 7.

Despite evidence for photoreceptor loss in NEAMD eyes, fewer than 10% of the macular counting sites showed significant loss of GCL neurons in five of six NEAMD eyes (Table 2), and there was no consistent location among the affected sites (Fig. 7A). In contrast, the number of counting sites with significant GCL neuron loss ranged from 42% to 96% in four EXAMD eyes and 8% in one EXAMD eye (Table 2). The locations with the most severe loss varied in the four most affected EXAMD eyes, with greater loss at distances more than 1 mm from the fovea in two eyes (Fig. 7B) and uniform loss in others. As expected from the density maps, the total number of GCL neurons in EXAMD eyes as a group was significantly lower than in control and NEAMD eyes, which did not differ from each other (Table 3). The mean number of GCL neurons in EXAMD eyes was 52.7% that of control eyes and 57.2% of NEAMD eyes (Table 3). However, NEAMD eyes did not differ significantly from control eyes.

## DISCUSSION

A major consideration for photoreceptor rescue techniques and electronic retinal prostheses for patients with photoreceptor degeneration is the state of the inner retinal layers.<sup>1</sup> In patients with AMD with severe photoreceptor loss, decreased input to the inner retina may result in transneuronal degeneration over time. The only study of GCL neurons in AMD known to us had an uncertain diagnosis of AMD, small sample size, and no control eyes.<sup>13</sup> Using a wholemount method to quantify GCL and photoreceptor topography<sup>18–20</sup> in histopathologically confirmed AMD donors, we determined the level of GCL neuron survival in relation to the level of photoreceptor loss in the same eyes. Our new findings are 47% loss of GCL neurons in end-stage cases of EXAMD but preservation of GCL neurons in NEAMD.

Despite massive photoreceptor loss in EXAMD, GCL neurons survived in relatively large numbers, perhaps because visual input to these cells had not been eliminated completely. Islands of photoreceptors persist adjacent to fibrovascular scars,<sup>12</sup> and photoreceptors in uninvolved areas may drive GCL neurons by way of retinal interneurons with very long processes (e.g., Reference 28). Within our EXAMD group, we were unable to determine when CNV was first present from the clinical records, and therefore we cannot relate the observed cell counts to the duration of neovascular disease.

TABLE 3. Total Cells

Total Cells	Control	NEAMD	EXAMD	Significance*
Cones, foveal	30.1 ± 3.9	29.1 ± 3.5	—	NS
Cones	322.5 ± 58.3	291.6 ± 37.8	—	NS
Rods	2269.4 ± 369.2	1971.0 ± 586.2	—	NS
GCL neurons	384.3 ± 58.7	353.2 ± 68.4	202.4 ± 77.9	0.00006

—, not determined. Counts are ×1000 (mean ± SD). NS, not significant.

\* *t*-Test, control vs. NEAMD eyes for photoreceptors; analysis of variance for GCL neurons.



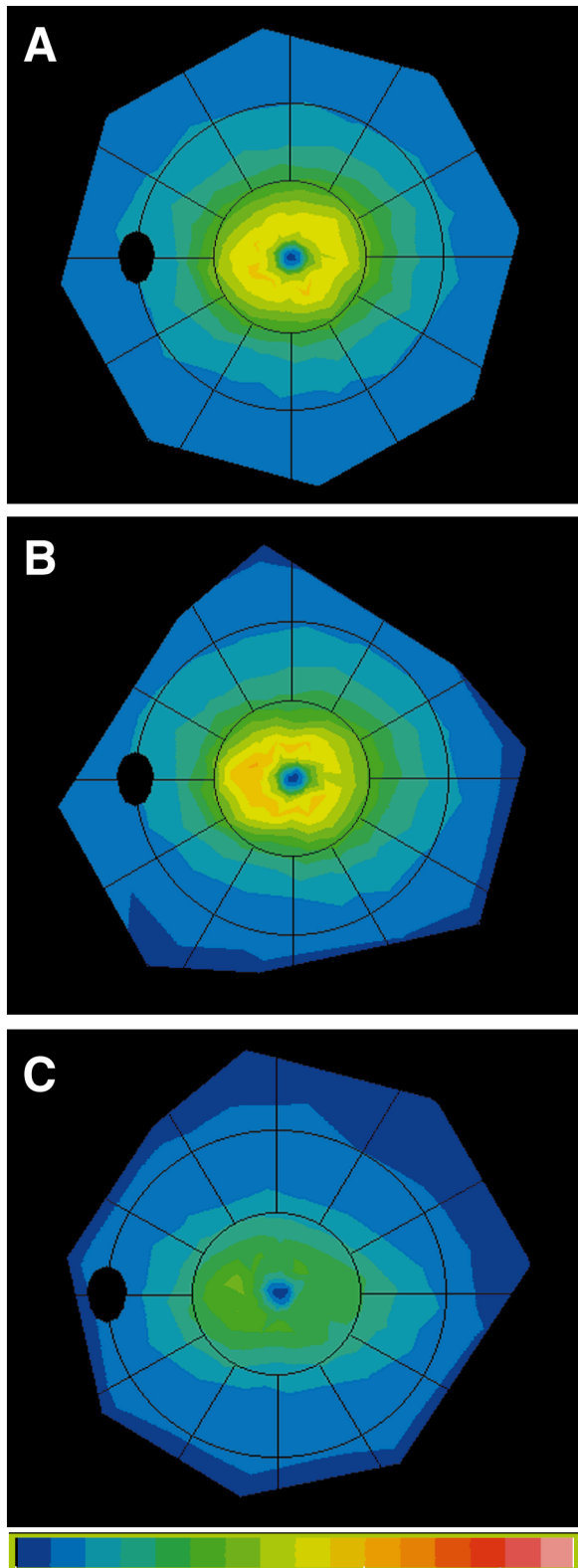


**FIGURE 6.** Mean density of GCL neurons in control eyes (A), NEAMD cases 1 through 6 (B), and EXAMD cases 7 through 11 (C). Maps were generated by resampling the maps of individual eyes at standard locations and are displayed as left eyes. Rings in the overlying grids are at intervals of 2 mm. The black oval is the optic disc. The color bar shows the spatial density (cells per square millimeter) of GCL neurons between 0 (dark blue) and 40,000 (pink) cells/mm<sup>2</sup> in intervals of 2,500 cells/mm<sup>2</sup>.

However, the only EXAMD eye in which GCL cell loss was undetectable (case 8) also had the smallest disciform scar (1.8 × 2.0 mm), suggesting that the maintained GCL neuron number in this eye was due to an earlier stage of CNV development. The exact number of displaced amacrine cells in the human macula is not known but is believed to be 10% or less on the basis of studies in nonhuman primates.<sup>26</sup> Therefore, a 47% reduction in the total neuron population of the GCL implies that at least three quarters of the missing neurons were ganglion cells. In contrast, the number of GCL neurons in NEAMD eyes as a group did not differ significantly from control eyes, probably because of the localized nature of photoreceptor loss in these eyes.

Even though more than half of GCL neurons remain in patients with end-stage EXAMD with fibrovascular macular scars, the implications of our results in these patients should be interpreted cautiously. Survival of neuronal cell bodies does not necessarily imply normal synaptic connections between neurons. Although our study documents the preservation of GCL neurons, we can address neither their functional status nor that of interneurons between photoreceptors and ganglion cells. In fact, evidence from animal models and human RP donors indicates that aberrant connections are present, in relation to the degree of photoreceptor loss.<sup>29-34</sup> Thus, the likelihood of the transplanted photoreceptors' connecting successfully with postreceptoral cells may progressively decrease with time. Moreover, synaptic sites on the desired target cells for transplants may be occupied by ectopic neurites extending from surviving cells.<sup>30,33,34</sup> Signal transmission in the synaptic layers may be degraded by alterations in the

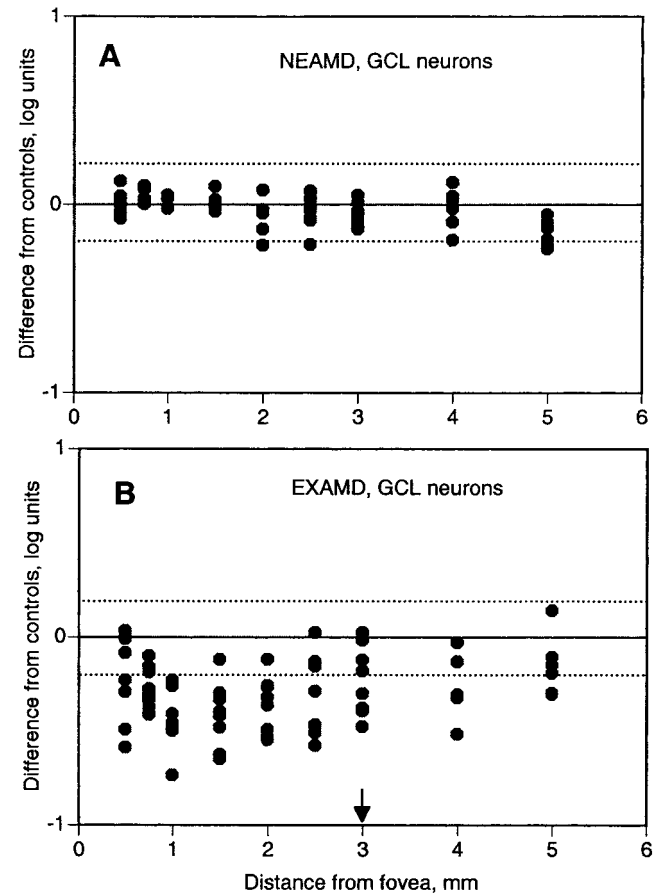


**FIGURE 7.** Loss of GCL neurons as a function of distance from the fovea in NEAMD case 4 (A) and in EXAMD case 9 (B). See Figure 4 for details.

local environment provided by Müller cells.<sup>32</sup> These responses to photoreceptor degeneration may help remaining neurons survive but do not necessarily produce normal visual function. Finally, GCL neurons can die subsequent to inner retinal vascular abnormalities in long-standing outer retinal degeneration,<sup>35,36</sup> and a vascular contribution to EXAMD-associated GCL neuron loss cannot yet be excluded. Together, these findings underscore the concept that interventions requiring an intact inner retina in patients with AMD are more likely to succeed if undertaken before substantial postreceptor reorganization occurs.

The implications of our results for the success of new treatments requiring intact inner retinal layers are potentially more positive in patients with early EXAMD. We did not detect a disease-related loss of GCL neurons in NEAMD eyes, and animal studies<sup>37-39</sup> suggest that GCs may be able to survive for some time after photoreceptor loss begins in elderly patients with EXAMD. Although the temporal relationship between the development of CNV and eventual cell loss is not known, it is likely that interventions initiated soon after CNV develops (e.g., photodynamic therapy<sup>40</sup> or translocation<sup>41</sup>) will benefit from significant numbers of GCL neurons. However, the success of photoreceptor rescue or replacement techniques in the presence of active CNV will probably require additional interventions to halt the harmful effects of existing CNV and to reduce the probability of CNV's recurrence. Further studies are necessary to clarify these issues.

Our findings for inner retinal survival after AMD-related photoreceptor loss can be compared to the findings in RP.<sup>3-5</sup> Similar to EXAMD eyes, RP eyes exhibit 50% to 75% GCL preservation, a positive correlation between the levels of photoreceptor and GCL neuron loss, and high individual variability. However, more macular GCL neurons remained in the eyes with AMD than in the eyes with RP, which had 48% and 30% of cells remaining in moderate and severe cases, respectively. This difference between AMD and RP results could be due to noncomparable disease stages or differences in disease course. With regard to disease stage, the last recorded visual acuities of NEAMD eyes in our study (with no detectable GCL loss) were much better than those in the moderate RP cases (>20/400), and the acuities of these EXAMD eyes (with 47% GCL loss) were better than those in the severe RP cases (no light perception). With regard to disease course, AMD begins late in life, whereas RP begins in adolescence or early adulthood.<sup>42</sup> Transneuronal degeneration in animal models is more severe when the initial insult occurs early in life.<sup>37,38</sup> Photoreceptor degeneration and its consequences are therefore more advanced by the time donor eyes with RP are typically available for histopathology.

In the course of characterizing photoreceptor loss in NEAMD and EXAMD eyes, we confirmed that a moderate diffuse loss of photoreceptors occurs in the parafovea of eyes with NEAMD.<sup>12</sup> The total number of macular photoreceptors in NEAMD eyes did not differ significantly from that in control eyes, however, because the loss was regional. Furthermore, it is possible that locally severe loss associated with individual drusen was not detectable with our systematic sampling methods. By counting cones and rods at the same locations, we determined the relative rate of cone and rod degeneration, a fundamental characteristic for any disease affecting photoreceptors. This study, in conjunction with our previous work,<sup>12</sup> demonstrated that macular rods were more severely affected than cones in three of four AMD eyes examined. Similarly, recent functional studies show that in 87% of patients with well-characterized NEAMD, the magnitude of mean scotopic sensitivity loss exceeds the magnitude of mean photopic sensitivity loss when compared with age-matched control patients.<sup>43</sup> These results indicate that tests of rod function may be

more sensitive indicators of early AMD than conventional photopic acuity tests for most patients. The mechanisms underlying the greater vulnerability of rods in AMD are currently unknown. One possibility is that the age- and disease-related accumulation of debris within Bruch's membrane and under the RPE impairs the transfer of essential nutrients and metabolites between the choriocapillaris and the RPE and photoreceptors.<sup>44</sup>

In summary, we have demonstrated a moderate, diffuse loss of photoreceptors in NEAMD and a severe loss of photoreceptors in EXAMD, both of which were dominated by the loss of rods. There was no detectable loss of GCL neurons in NEAMD. The number of neurons surviving in the GCL of EXAMD eyes may be sufficient to support signal transmission to the brain for experimental treatments of the outer retina.

### Acknowledgments

The authors thank the Alabama Eye Bank for timely retrieval of donor eyes, the Tissue Procurement Program of the University of Alabama at Birmingham Comprehensive Cancer Center for surgical specimens, C. Leigh Millican for technical assistance, and Gerald McGwin Jr. for statistical consultation.

### References

- Lund RD, Coffey PJ, Sauve Y, Lawrence JM. Intraretinal transplantation to prevent photoreceptor degeneration. *Ophthalmic Res.* 1997;29:305-319.
- Humayun M, de Juan E Jr, Dagnelie G, Greenberg R, Propst R, Phillips D. Visual perception elicited by electrical stimulation of retina in blind humans. *Arch Ophthalmol.* 1996;114:40-46.
- Stone JL, Barlow WE, Humayun MS, de Juan E Jr, Milam AH. Morphometric analysis of macular photoreceptors and ganglion cells in retinas with retinitis pigmentosa. *Arch Ophthalmol.* 1992;110:1634-1639.
- Santos A, Humayun M, de Juan E Jr. Preservation of the inner retina in retinitis pigmentosa: a morphometric analysis. *Arch Ophthalmol.* 1997;110:1634-1639.
- Humayun M, Prince M, de Juan E Jr, et al. Morphometric analysis of the extramacular retina from postmortem eyes with retinitis pigmentosa. *Invest Ophthalmol Vis Sci.* 1999;40:143-148.
- Inglehearn C. Molecular genetics of human retinal dystrophies. *Eye.* 1998;12:571-579.
- Van Soest S, Westerveld A, de Jong PTVM, Bleeker-Wagemakers EM, Bergen AAB. Retinitis pigmentosa: defined from a molecular point of view. *Surv Ophthalmol.* 1999;43:321-334.
- Klein R, Klein BEK, Linton KLP. Prevalence of age-related maculopathy. *Ophthalmology.* 1992;99:933-943.
- Mitchell P, Smith W, Attebo K, Wang JJ. Prevalence of age-related maculopathy in Australia: the Blue Mountains Eye Study. *Ophthalmology.* 1995;102:1450-1460.
- Vingerling JR, Dielemans I, Hofman A, et al. The prevalence of age-related maculopathy in the Rotterdam study. *Ophthalmology.* 1995;102:205-210.
- Bird AC, Bressler NM, Chisholm IH, et al. An international classification and grading system for age-related maculopathy and age-related macular degeneration. *Surv Ophthalmol.* 1995;39:367-374.
- Curcio CA, Medeiros NE, Millican CL. Photoreceptor loss in age-related macular degeneration. *Invest Ophthalmol Vis Sci.* 1996;37:1236-1249.
- Clarke S. Modular organization of human extrastriate visual cortex: evidence from cytochrome oxidase pattern in normal and macular degeneration cases. *Eur J Neurosci.* 1994;6:725-736.
- Barondes M, Pauleikhoff D, Chisholm IH, Minassian D, Bird AC. Bilaterality of drusen. *Br J Ophthalmol.* 1990;74:180-182.
- Spraul CW, Grossniklaus HE. Characteristics of drusen and Bruch's membrane in postmortem eyes with age-related macular degeneration. *Arch Ophthalmol.* 1997;115:267-273.



16. Wang JJ, Mitchell P, Smith W, Cumming RG. Bilateral involvement by age-related maculopathy lesions in a population. *Br J Ophthalmol*. 1998;82:743-747.
17. Curcio CA, Medeiros NE, Millican CL. The Alabama Age-Related Macular Degeneration Grading System for donor eyes. *Invest Ophthalmol Vis Sci*. 1998;39:1085-1096.
18. Curcio CA, Sloan KR, Kalina RE, Hendrickson AE. Human photoreceptor topography. *J Comp Neurol*. 1990;292:497-523.
19. Curcio CA, Allen KA. Topography of ganglion cells in human retina. *J Comp Neurol*. 1990;300:5-25.
20. Curcio CA, Drucker DN. Retinal ganglion cells in Alzheimer's disease and aging. *Ann Neurol*. 1993;33:248-257.
21. Curcio CA, Millican CL, Allen KA, Kalina RE. Aging of the human photoreceptor mosaic: evidence for selective vulnerability of rods in central retina. *Invest Ophthalmol Vis Sci*. 1993;34:3278-3296.
22. Ogden TE. Nerve fiber layer astrocytes of the primate retina: morphology, distribution, and density. *Invest Ophthalmol Vis Sci*. 1978;17:499-510.
23. Distler C, Weigel C, Hoffman K-P. Glia cells of the monkey retina, I: astrocytes. *J Comp Neurol*. 1993;333:134-147.
24. Ramirez JM, Trivino A, Ramirez AI, Salazar JJ, Garcia-Sanchez J. Immunohistochemical study of human retinal astroglia. *Vision Res*. 1994;34:1935-1946.
25. Ramirez JM, Trivino A, Ramirez AI, Salazar JJ, Garcia-Sanchez J. Structural specializations of human retinal glial cells. *Vision Res*. 1996;36:2029-2036.
26. Wässle H, Grünert U, Rohrenbeck J, Boycott BB. Cortical magnification factor and the retinal ganglion cell density in the primate. *Nature*. 1989;341:643-646.
27. Curcio CA, Owsley C, Skalka HW, Peters GE, Callahan MA, Long JA. Topography of retinal cells and visual sensitivity in the same human eyes [ARVO Abstract]. *Invest Ophthalmol Vis Sci*. 1993;34(4):S777. Abstract nr 375.
28. Dacey DM. The dopaminergic amacrine cell. *J Comp Neurol*. 1990;301:461-489.
29. Chu Y, Humphrey MF, Constable IJ. Horizontal cells of the normal and dystrophic rat retina: a wholemount study using immunolabeling for the 28-kDa calcium-binding protein. *Exp Eye Res*. 1993;57:141-148.
30. Li Z-L, Kljavin IJ, Milam AH. Rod photoreceptor neurite sprouting in retinitis pigmentosa. *J Neurosci*. 1995;15:5429-5438.
31. McCall MA, Gregg RG, Merriman K, Goto Y, Peachey NS, Stanford LR. Morphological and physiological consequences of the selective elimination of rod photoreceptors in transgenic mice. *Exp Eye Res*. 1996;63:35-50.
32. Fletcher EL, Kalloniatis M. Neurochemical architecture of the normal and degenerating rat retina. *J Comp Neurol*. 1996;376:343-360.
33. Peng Y-W, Hao Y, Petters RM, Wong F. Rhodopsin mutation induces ectopic cone-rod bipolar cell synaptic connections in transgenic swine. *Nat Neurosci*. 2000;3:1121-1127.
34. Fariss RN, Li Z-L, Milam AH. Abnormalities in rod photoreceptors and amacrine and horizontal cells in human retinas with retinitis pigmentosa. *Am J Ophthalmol*. 2000;129:214-223.
35. Li Z-Y, Possin DE, Milam AH. Histopathology of bone spicule pigmentation in retinitis pigmentosa. *Ophthalmology*. 1995;102:805-816.
36. Villegas-Perez MP, Lawrence JM, Vidal-Sanz M, LaVail MM, Lund RD. Ganglion cell loss in RCS rat retina: a result of compression of axons by contracting intraretinal vessels linked to the pigment epithelium. *J Comp Neurol*. 1998;392:58-77.
37. Grafstein B, Murray M, Ingoglia NA. Protein synthesis and axonal transport in retinal ganglion cells of mice lacking visual receptors. *Brain Res*. 1972;44:37-48.
38. Eisenfeld AJ, LaVail MM, LaVail JH. Assessment of possible transneuronal changes in the retina of rats with inherited retinal dystrophy: cell size, number, synapses, and axonal transport by retinal ganglion cells. *J Comp Neurol*. 1984;223:22-34.
39. Bush RA, Hawks KW, Sieving PA. Preservation of inner retinal responses in the aged Royal College of Surgeons rat. *Invest Ophthalmol Vis Sci*. 1995;36:2054-2062.
40. Bressler NM, Bressler SB. Photodynamic therapy with verteporfin (Visudyne): impact on ophthalmology and visual sciences. *Invest Ophthalmol Vis Sci*. 2000;41:624-628.
41. de Juan E Jr, Loewenstein A, Bressler NM, Alexander J. Translocation of the retina for management of subfoveal choroidal neovascularization, II: a preliminary report in humans. *Am J Ophthalmol*. 1998;125:635-646.
42. Heckenlively JR. *Retinitis Pigmentosa*. Philadelphia: JB Lippincott; 1988.
43. Owsley C, Jackson GR, Cideciyan AV, et al. Psychophysical evidence for rod vulnerability in age-related macular degeneration. *Invest Ophthalmol Vis Sci*. 2000;41:267-273.
44. Curcio CA, Owsley C, Jackson GR. Spare the rods, save the cones in aging and age-related maculopathy. *Invest Ophthalmol Vis Sci*. 2000;41:2015-2018.